JOURNAL OF OPTOELECTRONICS AND ADVANCED MATERIALS Vol. 9, No. 11, November 2007, p. 3609 - 3613

Hydroxyapatite-iron oxide bioceramic prepared using nano-size powders

D. PREDOI*, M. BARSAN[a], E. ANDRONESCU[a], R.A. VATASESCU-BALCAN[b], M. COSTACHE[b]
National Institute of Materials Physics, P.O. Box. MG 07, 077125, Magurele, Romania,
[a]*University POLITEHNICA of Bucharest, Faculty of Applied Chemistry and Materials Science, Department of Science and Engineering of Oxide Materials and Nanomaterials, Bucharest, Romania*
1 – 7, Polizu Street, 011061, PO – BOX 12-134, Bucharest 1, Romania
[b]*Molecular Biology Center, University of Bucharest, 91-95 Splaiul Independenţei, 76201, Bucharest 5, Romania*

The hydroxyapatite (HAp) is an important material for orthopedics and dentistry applications. In the present study a simple method was tried for added the iron oxide nanoparticles into HAp so as to establish and induce a biocompatibility. In the research the mechanism of the coated of iron oxide with HAp would also be described by the analysis of X-ray diffractometer, scanning electron microscope and Fourier transformation infrared. Osteoblast cells were permanent monitored to detect any possible influence due to samples that might alter the cell growth, viability and proliferation.

(Received August 2, 2007; accepted November 1, 2007)

Keywords: Nanoparticles, Iron oxyde, Hydroxyapatite, Bioceramic, Cell culture

1. Introduction

Inorganic composites are of special interest for biomedical applications such as in dental and bone implants wherein the ability to modulate the morphology and size of the inorganic crystals is important. One interesting possibility to control the size of inorganic crystals is to grow them on nanoparticles [1]. In the last years bioactive materials such as hydroxyapatite ceramics has been studied for clinical use as a bone-graft substitute and a coating for prostheses as well as to fill bone defects [2-4].HA has various applications in orthopaedic surgery such as in bone defects resulting from severe fractures, spinal surgery and arthroplasty [5-7]. The intrinsic architecture of the HA was preserved on radiographs, but that the margins had become indistinct, suggesting partial biodegradation of the material.

In this study, iron oxide nanoparticles were synthesized by coprecipitation method. The iron oxide powders were introduced in hydroxyapatite (HAp) and sintering at 800^0C. In addition, the structural properties iron oxide nanoparticles coated with hydroxyapatite were studied using X-ray diffraction, transmission electron microscopy (MET), Scanning Electron Microscopy (SEM), IR spectrometry and DTA / TG analysis. This article presents results from cytotoxicity assays of cells culture.

2. Experimental

2.1 Sample preparation

Iron-oxide nanoparticles were prepared according to the following procedure: ferrous chloride tetrahydrate ($FeCl_2 \cdot 4H_2O$) in 2M HCl and ferric chloride hexahydratate ($FeCl_3 \cdot 6H_2O$) were mixed at room temperature (Fe^{2+}/Fe^{3+} = ½). The mixture was dropped into 200 ml of 1.5M NaOH solution under vigorous stirred for about 60 min. The resulting precipitate was insolated in the magnetic field and the supernatant was removed from the precipitate by decantation. Purified deionisated water was added to the precipitate and the solution decanted after centrifugation at 8000 rot/min. After repeating the lost procedure two times, 200 ml of 0.02M HCl solution was added to the precipitate with continuous agitation. The product was separated by centrifugation (8000 rpm) and dried at 40^0C.

Two series of samples were prepared in the system hydroxyapatite (HAp), iron-oxide nanoparticles. Two different compositions were chosen as presented in Table 1.

Powders of HAp and iron oxide nanoparticles were milled for 5 hours at 250 rot / min in a dried environment. The obtained powders were then thermally treated at 800 ^{o}C for 2 hours (sample M11 and sample M13).

Table 1. The composition of the two samples.

Sample	HAp (weight %)	Fe_3O_4 (weight %)
M11	90	10
M13	80	20

2.2 Sample characterization

The samples were characterized by X-ray diffraction (XRD) with a Philips PW1050 X- ray powder diffractometer using CuK_α incident radiation. An estimation of crystallite sizes was done from the width of the diffraction using the Scherrer formula. Transmission electron microscopy (TEM) experiments were performed with a JEOL 2000FX operating at an accelerating voltage of 200 kV. Sample for TEM were performed on copper grids coated with a carbon support film by evaporating a drop of particles dispersions.

Using a Scanning Electron Microscope with, type HITACHI S2600N with EDAX / 2001 device, operating at 25kV in vacuum, the structure and morphology of the samples were studied. The SEM studies were performed on powder samples.

IR spectroscopic studies were performed in the range 1800-400 cm^{-1} using a FTIR Spectrum BX spectrometer. Samples dehydrated at room temperature were pelleted with dried KBr. On the powders, Differential Thermal Analysis and Thermal Gravimetric Analysis were performed using the Shimadzu DTG-TA-50 and DTA 50 analyser, in the 25 – 1000 ^oC temperature range, weight detection ±20- ± 200 mg, air environment, reference made of Al_2O_3.

2.3 Biological test

2.3.1 Cell culture

Osteoblasts were grown in Dulbecco Modified Eagle's Medium (DMEM) supplied with 10% fetal bovine serum, DMEM sodium pyruvate, 2% glutamine and antibiotic mix. Medium compounds were purchased from Gibco (UK). The cells were incubated at 37°C, 5% CO_2 and the split was performed using tripsin-EDTA solution 1x (Sigma-Aldrich) and phosphate-buffered saline (PBS) from Gibco.

Osteoblasts used to determine the cell proliferation, viability and citotoxicity interaction with M11 and M13 bioceramics has been obtained from the upper part of the patient's femur. These patients undergo the surgery intervention in arthritis disease when the haunch articulation is removing.

Primary osteoblast culture from bone explants was designed according to Gallagher et al (1996) protocol [8]. The pieces from bone tissue are transferred into a sterile recipient with PBS. Obtained tissue is detached from soft conjunctive tissue of the external bone area. The tissue is rinsed in sterile PBS and removed in Petri dishes which contain a small volume of sterile PBS proportionally to the size of the pieces.

Next step was to place the explant fragments in DMEM with antibiotics supply, washing successively with antibiotic solutions, cultivated in DMEM medium supplied with 15% Bovine Serum Albumin (BSA), 2% glutamine and buffered with natrium bicarbonate.

The first osteoblasts from explants arised after 7-10 days of incubation (5% CO_2 atmosphere, T=37^oC) and were suitable for split after 4-6 weeks; after the second passage, the culture contains strictly osteoblast cells. Subsequent splits were performed at confluence (2 x 10^6 cells/plate) in about 10 days, with a 1:3 ratio. Confluent cultures have been treated with trypsin for 2-3 min and then centrifuged at 1,500 rpm for 10 min. Cells were re-suspended in minimal DMEM volume, counted with Burker-Turk chamber and evenly distributed on sterile supports, previously treated with polylisine.

2.3.2 Cell viability

Biocompatibility test of the M11 and M13 substrate (bioceramics) has been made using primary osteoblast cell line. After osteoblast culture achievement, the cells were treated with trypsin 0.05% and splitted in 35/35 mm Petri dish.

Cells were seeded at a density of 10^5 cells/ml in Petri dish and incubated with M11 and M13 bioceramics for 48 hours. The cell viability was determined by MTT (3-(4, 5-dimethylthiazol-2-yl)-2, 5-diphenyltetrazolium bromide) reduction test. The cells were incubated (5% CO_2 atmosphere, T=37^oC) for 4h with MTT (0.1 mg/ml).

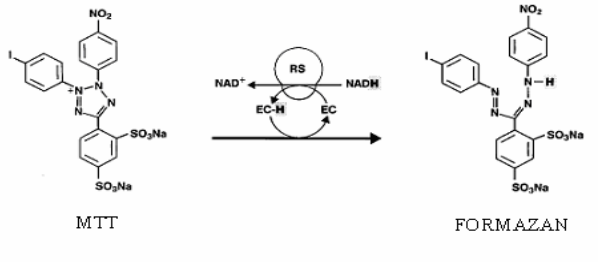

Fig. 1. MTT is reduced to formazan in mitochondria of the cells.

The viability cell number is directly proportional to the production of formazan. The isopropanol was added to dissolve the insoluble purple formazan product into a colored solution. The absorbance was quantified by measuring the wavelength at 595 nm by TECAN spectrophotometer.

3. Results and discussion

XRD patterns of the iron oxide nanoparticles (Fe_xO_y), commercial hydroxyapatite (HAp) and commercial hydroxyapatite with different iron oxide additions (M11 and M13) are shown in Fig. 2a and Fig. 2b. The XRD spectra, for samples M11 and M13 shows the phase peaks corresponding to iron oxide and a mixture of HAp and β- TCP (β-tricalcium phosphate). This confirms that the stoichiometry of HAp very much determines its thermal stability and non-stoichiometric HAp readily decompose to β- TCP upon heat- treatment to 1000^0C, as is known in calcium phosphates literature [9]. The position and relative intensity of all diffraction peaks match well with those of the iron oxide powder and to a crystalline hydroxyapatite.

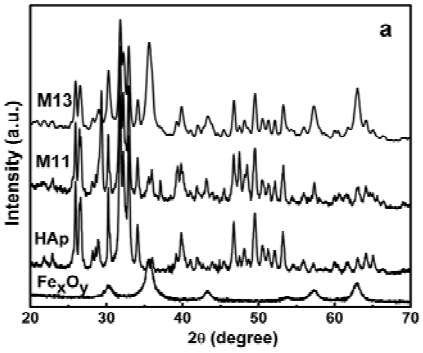

Fig. 2a. X-Ray diffraction pattern of Fe_xO_y, HAp and sample M11 and sample M13.

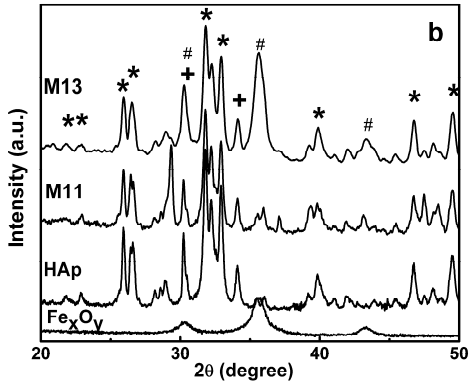

Fig. 2b. X-Ray diffraction pattern of Fe_xO_y, HAp and sample M11 and sample M13 in the range of 20-50 degree (: HAp peaks, +: β-TCP peaks, #: Fe_xO_y peaks).*

Fig. 3 shows a TEM image that was used to determine particle size and morphology for iron oxide nanoparticles. The size of the sample M11 is lesser than that of the sample M13. The distribution of iron oxide nanoparticles is uniform and they are coated with HAp grains.

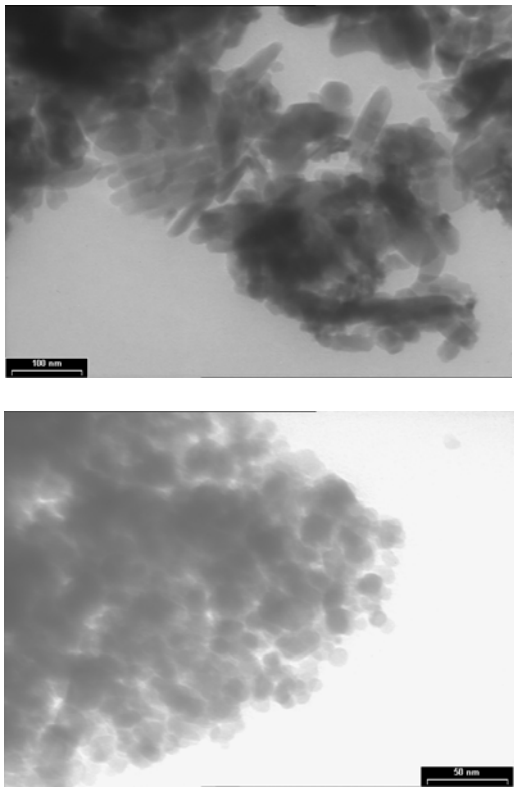

Fig. 3. Transmission electron microscopy (MET) of the samples M11 and M13.

Results of the SEM analysis are shown in Fig. 4. We can notice that the scanning electron photomicrograph of the samples revealed that the iron oxide nanoparticles seemed to be mostly incorporated in the hydroxyapatite spheres and no free magnetic particles were discernable in SEM.

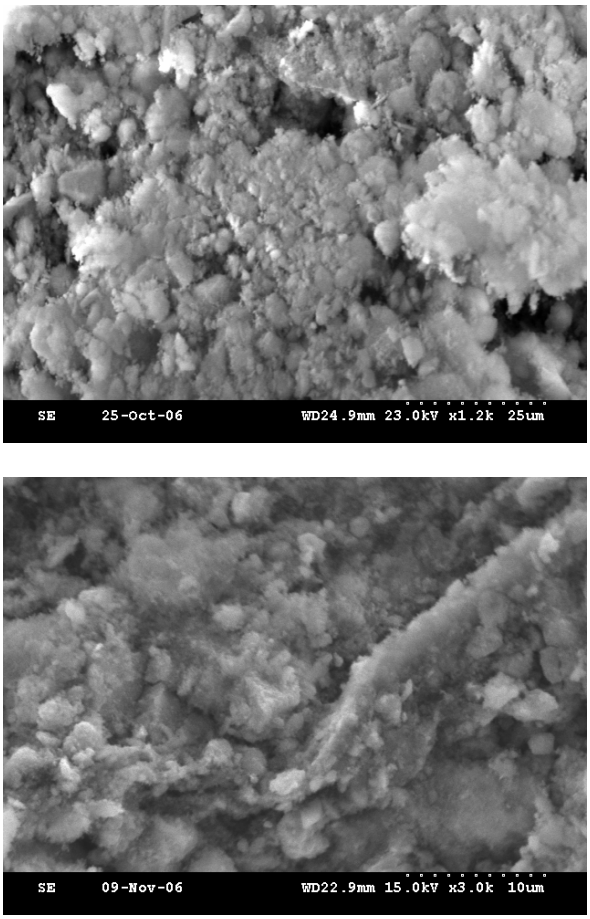

Fig. 4. The SEM micrographs of samples M13 and M23 powder.

Fig. 5 shows the DTA/TGA plot of the sample M11 and sample M13 by conducting thermal analysis in air. The weight loss between 100 ^{0}C and 400 ^{0}C contributes to the loss of lattice water 10-12]. The gradual decrease in weight from 400 ^{0}C to 800 ^{0}C is probably a result of the show elimination of the carbonate groups linked to HAp, the presence of which has been confirmed by FTIR analysis discussed later [13].The decomposition of HAp is promoted by the presence of minute impurities or the non-stoichiometry of the HAp powder as reported according to the reaction [14]:

$$Ca_{10}(PO_4)_6(OH)_2 \rightarrow 3Ca_3(PO_4)_2 + CaO + H_2O$$

In our samples it was observed that the percentage of weight loss in 2% for sample M13 and 1.46% for sample M23.The differences in weight loss of sample M13 and sample M23 shows that the weight loss is determinate by size of iron oxide addition.

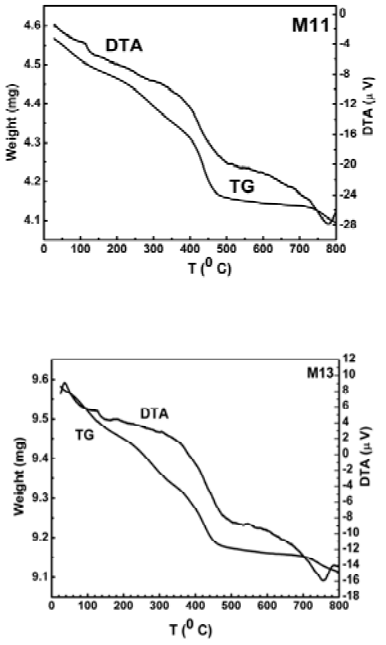

Fig. 5. The DTA/TGA evolution curves for sample M11 and M13.

The attachment of the HAp on the particle surface was confirmed by FTIR spectroscopy. The analyses of the FTIR vibrations band were recorded in the range of 2000-400 cm^{-1} for all the samples. The infrared spectra of the sample H1 and H2 (Fig. 6) show the vibration modes of Fe_3O_4 and of HAp. In this specra, the characteristic bands of HAp are observed [15-17].

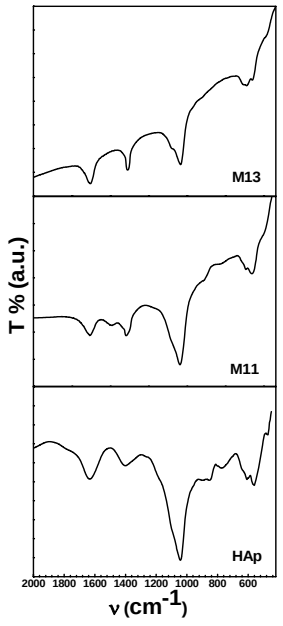

Fig. 6. IR spectra of hydroxyapatite (HAp) and iron oxide coated with hydroxyapatite (samples M11 and M13).

The bands at 550-600 cm^{-1} can be attributed to the M_{Th}-O-M_{Oh} (ν1) and to the PO_4^{3-} ions (ν4). The shoulder at 960 cm^{-1} (ν1) and the band at 1040 cm^{-1} (ν3) can be attributed to the PO_4^{3-} ions. Vibrations associated to the vibrations of hydrogen-bonded water molecules adsorbed on the surface are detected by the band 1640. The presence of carbon modes in commercial sample is an indication that carbon is also an impurity in this sample from the preparation process, which is not detected in the X-ray.

Cell membrane is not disrupted in response to iron oxide nanoparticles coated with hydroxyapatite producing a large cell extension.

MTT assay is a laboratory test and a standard colorimetric assay (an assay which measures changes in colour) for measuring cellular proliferation (cell growth). It is used to determine cytotoxicity of potential medicinal agents and other toxic materials.

Yellow MTT (3-(4,5-Dimethylthiazol-2-yl)-2,5-diphenyltetrazolium bromide, a tetrazole) is reduced to purple formazan in the mitochondria of living cells. A solubilization solution (isopropanol) is added to dissolve the insoluble purple formazan product into a colored solution. The absorbance of this colored solution can be quantified by measuring at a certain wavelength (usually between 500 and 600 nm) by a spectrophotometer.

This reduction takes place only when mitochondrial reductase enzymes are active, and therefore conversion is directly related to the number of viable cells. When the amount of purple formazan produced by cells treated with an agent is compared with the amount of formazan produced by untreated control cells, the effectiveness of the agent in causing death of cells can be deduced, through the production of a dose-response curve.

Osteoblast cells were permanent monitored to detect any possible influence due to M11 and M13 bioceramics that might alter the cell growth, viability and proliferation. This study represents one of the key-step in cell biology, mitochondrial dehydrogenases being essential.

Table 2. Absorbance values at 595 nm.

Samples	DO_{595nm}	Viability (%)
Control	0.336333	100
M11	0.061567	18.30525
M13	0.1064	31.63528

The results obtained after MTT assay have revealed (Table 2) as we expected, the fact that control sample has the greatest value (0.336). This value is also established by the high intensity of the color (deep purple) in control due to the amount of formazan produced by cells.

Our data indicate that osteoblast cells' growing on M13 substrate presented a higher peak (0.1064), comparing to those incubate on M11 support which shown a smaller peak (0.0615). The study reveals that osteoblast cells' growing on M11 and M13 bioceramic for 48 hours presented smaller peaks, comparing to control (Table 2). .

Table 3. MTT assay in osteoblast cell's growing with M11 and M13 bioceramics.

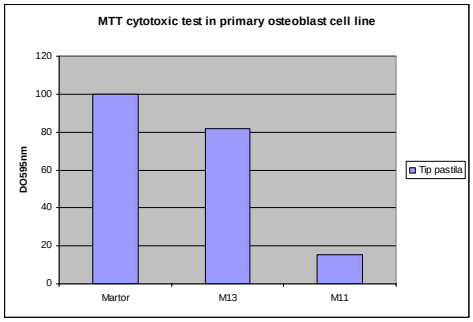

Cells growing on M13 support shown a diminish viability (31.63%), comparing to control (100%). In the same manner, the osteoblast cells incubated with M11 substrate presented a growth inhibition and the decrease of viability (18.30%), relating to control (Table 2, Table 3). This effect might be due to cells interaction with bioceramic.

The micro cells configurations (bioceramic) made by hydroxyapatite doped with nanometric magnetite could be a suitable support for osteoblast cells adhesion and proliferation without any modification of their structure and function.

MTT test demonstrate that cells' growing on M12 substrate can alter growth parameters, leading to a decrease of proliferation and viability comparing to control. The results we obtained reveal that M12 bioceramic is not very suitable for adherence and cell proliferation. Also, the exposure period could be an important factor in osteoblast cell's growing.

4. Conclusions

Iron oxide nanoparticles with have been synthesized by co-precipitation. The commercial hydroxyapatite with different iron oxide additions have been prepared by ball-milling and the obtained powders were then thermally treated at 800^0C. The properties of iron oxide nanoparticles coated with hydroxyapatite have been investigated. The iron oxide nanoparticles seemed to be mostly incorporated in the hydroxyapatite spheres and no free magnetic particles were discernable in SEM. Moreover the adsorption of the hydroxyapatite on iron oxide nanoparticles surface were evidenced by IR spectroscopy and were confirmed by thermal analysis.

The micro cells configurations (bioceramics) made by hydroxyl apatite doped with nanometric magnetite could be a suitable support for osteoblast cells adhesion and proliferation without any modification of their structure and function.

MTT test demonstrate that cells' growing on M11 and M13 substrates can alter growth parameters, leading to a decrease of proliferation and viability comparing to control. The results we obtained reveal that cell's viability on M13 support is near two fold greater than those observed on M11 substrate. We can conclude M13 substrate is a support more suitable for adherence and cell proliferation. Also, the exposure period could be an important factor in osteoblast cell's growing.

Acknowledgements

This work was financially supported by Science and Technology Ministery of Romania (Project CEEX_24/2005 and the Project CEEX_150/2006 VIASAN Program). We gratefully acknowledge Institut de Chimie de la Matière Condensée de Bordeaux for the use of theirs laboratories in the sample characterizations.

References

[1] D. Rautaray, S. Mandal , M. Sastry **21**(11), 5185 (2005).
[2] K. Ohura, M. Ikenaga, T. Nakamura, T. Yamamuro, Y. Ebisava,T. Kokubo, Y. Kotoura, M. Oka, Bioceramics, **3**, 225 (1992).
[3] Y. Ebisava, T. Kokubo, K. Ohura, T. Yamamuro, J. Mater. Sci: Mater Med **4**, 225 (1993).
[4] M. Ikenaga, K. Ohura, T. Yamamuro, Y. Kotoura, M. Oka, T. Kokubo, J. Orthop. Res. **11**, 849 (1993).
[5] Y. Ebisava, F. MiYaji, T. Kokubo, K. Ohura, T. Nakamura, J. Biomater, **18**, 1277 (1997).
[6] K. Takegami, T. Sano, H. Wakabayashi, J. Sodona, T. Yamazaki, S. Morita, T. Shibuya, A. Uchida, J. Biomed. Mater. Res. , **43**, 210 (1998).
[7] U. Gross, V. Strunz, J. Biomed. Mater. Res. **19**, 251 (1985).
[8] A.J. Gallagher, R. Gundle, N.J.Beresford, Isolation and culture of bone forming cells (osteoblasts) from human bone, Human Cell Culture Protocols (Jones, E.G., eds.), 233-263, (1996).
[9] N. Kivrak, A. Tas Cuneyt, J. Am Ceram Soc. **81**(9), 2245 (1998).
[10] W. Suchanek, Y. Masahiro, J. Mater. Res. **13**(1), 94 (1998).
[11] W. L. Suchanek, P. Shuk, K. Byrappa, R. E. Riman, K. S. Tenhuisen, V.F. Janas, Biomaterials **23**, 699 (2002).
[12] P. N. Kumta, C. Sfeir, D. H. Lee, D. Olton, D. Choi, Acta Biomaterialia **1**, 65 (2005).
[13] P.N. Kumta, C. Sfeir, D.H. Lee, D. Olton, D. Choi, acta Biomaterialia **1**, 65 (2005).
[14] N. Kivrak, A. Cuneyt Tas, J. Am. Ceram. Soc **81**(9), 2245 (1998).
[15] I.F. Vasconcelos, J. Mater. Sci. **36**, 587 (2001).
[16] M.N. Taravel, Biomaterials, **16**(11), 865 (1995).
[17] C.C. Silva, H.G. B. Rocha, F.N.A. Freire, M.R.P. Santos, K.D.A. Saboia, J.C. Goes, A.S.B. Sombra, Materials Chemistry and Physics **92**, 260 (2005).

*Corresponding author: dpredoi_68@yahoo.com